Surface coastal circulation patterns by *in-situ* detection of Lagrangian Coherent Structures

F. Nencioli,[1] F. d'Ovidio,[2] A. M. Doglioli,[1] and A. A. Petrenko[1]

[1]Aix-Marseille Université; CNRS; IRD; LOPB-UMR 6535, Laboratoire d'Océanographie Physique et Biogéochimique, OSU/Centre d'Océanologie de Marseille, France

[2]Laboratoire dOcéanographie et du Climat: Experimentation et Approches Numeriques, IPSL, Paris, France

Coastal transport and cross-shelf exchanges are important factors in controlling the dispersal of human and river discharged pollutants, as well as the advection of nutrients and larvae. Altimetry-based Lagrangian techniques provide accurate information on horizontal transport in the open ocean but are unreliable close to the coast. In order to circumvent this problem, during the LAgrangian Transport EXperiment 2010 campaign (Latex10, 1-24 September 2010) transport structures in the western Gulf of Lion were investigated with an adaptive sampling strategy, combining satellite data, ship-based ADCP measurements, and iterative Lagrangian drifter releases. The sampling strategy was able to identify errors in the surface transport patterns derived from altimetry, and to track with *in-situ* observations attractive and repelling Lagrangian coherent structures for a period of 12 days. The structures maintained a corridor ∼10 km-wide, roughly parallel to the coast, along which waters from the continental shelf leave the gulf. This is confirmed by high-resolution SST imagery. The use of this sampling strategy to explore surface transport structures may provide important information for the environmental management of coastal regions, and may serve for validating future coastal altimetric products.

1. Introduction

Coastal regions are a key environment for human activities, as they provide a wide variety of services and resources. In the last decades, coastal environments have been rapidly degrading under the pressure of human impact and global change and therefore a correct management of their ecological resources has become crucial for their preservation [*EEA*, 2010]. Coastal transport and cross-shelf exchanges control not only the transfer of heat and momentum, but also the advection of nutrients and larvae, as well as the dispersal of anthropogenic and river-discharged pollutants [*Huthnance*, 1995; *Largier*, 2003]. For these reasons, they represent important factors in regulating the ecological and biogeochemical conditions of coastal regions.

In recent years, Lagrangian techniques have become increasingly important for the analysis of horizontal mixing and transport properties in the ocean. Two of the most commonly used Lagrangian diagnostics are the Finite Time Lyapunov Exponent (FTLE) [*Haller and Yuan*, 2000], and the Finite Size Lyapunov Exponent (FSLE) [*Aurell et al.*, 1997]. Both methods measure the separation rate of the trajectories of close initial particles, and can be applied for two complementary goals: quantifying dispersion processes [i.e. *Waugh and Abraham*, 2008; *Haza et al.*, 2010; *Lumpkin and Elipot*, 2010; *Schroeder et al.*, 2011], or mapping Lagrangian Coherent Structures [LCSs; *Haller and Yuan*, 2000; *d'Ovidio et al.*, 2004; *Olascoaga et al.*, 2006; *Lehahn et al.*, 2007; *Beron-Vera et al.*, 2008; *Haller*, 2011]. Repulsive and attractive LCSs are associated with hyperbolic points of the flow, and provide direct information on transport and mixing patterns [*Mancho et al.*, 2008]: particles spread while moving toward hyperbolic points along repelling LCSs, whereas they

aggregate while moving away from hyperbolic points along attracting LCSs, which thus represent transport barriers [*Lehahn et al.*, 2007; *Haller*, 2011]. The spatial organization of these structures has a large impact on the coastal environment, not only because they influence the dispersion of any tracer in the water, but also because, by separating dynamically distinct regions of the flow, they can define fluid dynamical niches which contribute to the structuring of marine ecosystems [*d'Ovidio et al.*, 2010] and top predator distribution [*Kai et al.*, 2009; *Cotté et al.*, 2011].

FSLE and FTLE can be applied to geostrophic velocity fields derived from satellite altimetry in order to reliably detect LCSs in the open ocean. Several studies have confirmed the tight correlation between the detected structures and advected tracers. These include: Sea Surface Temperature (SST) [*Abraham and Bowen*, 2002; *d'Ovidio et al.*, 2009], surface chlorophyll concentrations [*Lehahn et al.*, 2007], and the oil from the recent spill in the Gulf of Mexico (this study used velocity fields from an ocean forecast model) [*Mezić et al.*, 2010]. This altimetry-based approach cannot be applied reliably in coastal regions, where the different ageostrophic dynamics induced by lateral and bottom boundaries and nearshore forcings [*Csanady*, 1982], insufficient sampling, presence of land mass and inaccuracy of geophysical corrections [*Bouffard et al.*, 2008], represent critical limiting factors for altimetry.

In this letter we propose a way for circumventing this problem, by detecting LCSs directly with an iterative, *in-situ* sampling strategy. This strategy was used during the LAgrangian Transport EXperiment 2010 campaign (Latex10) conducted from September 1 to 24 in the western part of the Gulf of Lion (hereafter GoL) aboard the *R/V Le Suroît*

and the *R/V Téthys II*. To our knowledge, this is the first time that both attracting and repelling LCSs were successfully detected and tracked in the ocean from *in-situ* observations, without reliable information on the velocity field from remote sensing (previous studies like *Shadden et al.* [2009] and *Haza et al.* [2010] had reliable velocity fields from HF radar observations, whereas *Beron-Vera et al.* [2008] and *Resplandy et al.* [2009] from satellite altimetry).

2. Data and Methods

The adaptive sampling strategy adopted during Latex10 combined satellite altimetry data, ship-based Acoustic Current Doppler Profiler (ADCP) measurements, and iterative Lagrangian drifter releases. A first-guess organization of the LCSs was first deducted from altimetry-derived FSLEs, although errors were expected due to the well known unreliability of altimetry in coastal regions. Following *Resplandy et al.* [2009] and *Haza et al.* [2010], which showed that drifter trajectories are strongly associated with LCSs, three arrays of drifters were released at intervals of few days to obtain *in-situ* estimates of the structures. The deployment position and the spatial configuration of each array was chosen on the basis of the outcome of the previous launch, at few days interval. Drifter data were then integrated in near-real time with ADCP mapping after each subsequent deployment in order to refine the synoptic picture of the transport structures.

A total of 14 Technocean Surface Velocity Program (SVP) subsurface drifters were used. Each drifter was tethered to a holey-sock drogue centered at 15 m depth (except 4 which had the drogue centered at 50 m), and equipped with a GPS transmitter which communicated its position every 30 minutes. The drifters were deployed in arrays of

varying number, each array corresponding to one of the 3 Lyapunov experiments (hereafter Lyap01, Lyap02, Lyap03) described in Section 3. Some of the drifters were recovered during the campaign and then re-deployed within a different array.

The ADCP data used for the *in-situ* mapping were collected with a VMBB-150 kHz ADCP mounted on the *R/V Téthys II*. Following *Petrenko et al.* [2005], the instrument was configured for recording 1 minute ensemble averages with a vertical resolution of 4 m from 11 to 247 m of depth.

Geostrophic velocities from the AVISO dataset (1/8° resolution over the Mediterranean basin; http://www.aviso.oceanobs.com) were used for the FSLE analysis. Detailed description of processing and corrections of AVISO satellite altimetry can be found in *SSALTO/DUACS User Handbook* [2010]. During the campaign, daily maps of FSLE were produced from Real-Time Maps of Absolute Dynamic Topography (RT-MADT). The maps presented in this letter were computed post-campaign using the further corrected Near Real-Time Maps of Absolute Topography (NRT-MADT). The two products did not evidence large differences in the area of study.

Altimetry-based FSLEs were computed with the method proposed by *d'Ovidio et al.* [2004]. Parameters were chosen as in *d'Ovidio et al.* [2009] with the exception of the final separation that has been set to 0.1° (∼10 km) in order to shorten advection times and minimize the number of particle trajectories that reach the coast. During the campaign, only attracting LCSs (backward integration) could be identified using time varying velocity fields. Positions of repelling LCSs (forward integration) were approximately estimated using a single snapshot of the velocity field (the most recent one). The repelling LCSs

presented in this letter were computed post-cruise, when velocity fields up to 60 days after the end of Latex10 were available.

Our iterative strategy for reconstructing transport structures was based on the following steps: (i) use altimetry for a first-guess of LCS positions; (ii) release a first array in the vicinity of LCS candidate positions; (iii) re-estimate the LCS positions on the basis of the drifter trajectories, relative dispersion and ADCP data; (iv) repeat from step (ii).

3. Results

The prominent feature of the GoL's circulation is the Northern Current (NC), a strong quasi-geostrophic current flowing from East to West along the continental slope [*Millot*, 1990]. The NC is visible in AVISO velocities on September 14 (Figure 1 Left). On the continental shelf, the velocity field indicates the presence of a typical anticyclonic circulation in the western part [*Estournel et al.*, 2003], and a smaller cyclonic structure further North-East. Repelling (red) and attracting (blue) LCSs are associated with the NC, confirming its important role as cross-shelf transport barrier [*Millot*, 1990]. These LCSs extend from the hyperbolic point identified by the intersection of repelling and attracting structures at $\sim$4°05′E, 42°55′N to the East of Cape Creus (3°20′E, 42°20′N). The LCSs along the coastline, characterized by step-like features, are artifacts resulting from the land-sea masking of the velocity field which affects the relative dispersion of particles nearshore. The effect is most likely enhanced by the strong cross-shelf components of velocity near the coastline. The four "Lyap01" drifters on the continental shelf where deployed on September 12 from the *R/V Le Suroît* at a distance of $\sim$5 km from each other. The other three (equipped

with 50m-deep drogues) were deployed on September 1 at 42°57′N between 5°45′ and 5°48′E, and then advected to their initial position in Figure 1 Left by the NC.

Trajectories parallel to the continental slope confirm the presence of the NC (Figure 1 Right). This is further supported by ADCP velocities, which reach their maximum magnitude across the continental slope. The trajectories identify the *in-situ* positions of the eastern (repelling) and southern (attracting) LCSs, which are similar to the ones obtained from satellite derived FSLEs, although more offshore than in Figure 1 Left. However, *in-situ* measurements indicate the presence of a western (repelling) LCS on the continental shelf not evidenced by satellite derived FSLE. Furthermore, ADCP velocities on the shelf seem to indicate a cyclonic circulation opposite to the AVISO field. From "Lyap01" data only, it is not possible to determine if the observed differences are only related to an inaccurate location of the structures in the AVISO field, or if they are due to dynamical features not detected by satellite altimetry. The position of the northern (attracting) LCS is derived from the results of the "Lyap02" and "Lyap03" deployments (Figures 2 and 3). The point of intersection of the LCSs at 4°E, 42°40′N gives a rough estimate of the *in-situ* position of the hyperbolic point. The area around the point is characterized by a local minimum of ADCP velocities. This supports the estimated position, since, although hyperbolic points are stationary only in the limiting case of time-independent velocity fields, their translational speed should be small compared to the mean advection velocities.

AVISO velocities and satellite derived FSLEs did not show large variations in the days after the "Lyap01" deployment (Figure 2 Left). Therefore, it was decided to further in-

vestigate the LCSs along the continental slope by deploying the five "Lyap02" drifters along a perpendicular section across them, with initial spacing between ∼3 to ∼7 km. Initial trajectories are consistent with the presence of a LCS (Figure 2 Right). However, their north-southward spreading along ∼3°40′E indicates the presence of attracting LCSs not evidenced by satellite derived FSLEs. The trajectory pattern is a typical example of particle dispersion from repelling towards attracting LCSs, and allows to accurately identify their position. On the other hand, the position of the western LCS on the continental shelf is estimated from "Lyap01" and "Lyap03" data (Figure 1 and 3, respectively). The position of the hyperbolic point is ∼3°40′E, ∼42°30′N. Thus, in the 6 days between the two deployments, it migrated by roughly 1/3° to the south-west, with an average translation speed of ∼5 cm sec^{-1}.

The drifter trajectories on the continental shelf indicate that *in-situ* mean currents were opposite to the anticyclonic circulation detected by AVISO velocities. ADCP velocities also show some limitations in representing mean current directions, due to the presence of strong near inertial oscillations (NIO), typical for the area [*Petrenko et al.*, 2005]. NIO are evidenced by the loops characterizing drifter trajectories, as well as by the rotation of the velocity vectors along the latitudinal transect at 3°50′E, which was sampled on two successive passages within few hours from each other (Figure 2, right). Strong NIO can influence the direction of instantaneous velocities, which therefore not always represent the direction of the mean transport. This can be observed around the northern LCS, where ADCP vectors are opposite to the drifter trajectories.

Between September 20 and 24, AVISO velocities remained similar to the previous two deployments (Figure 3 Left). The deployment of the five "Lyap03" drifters (initial spacing between the drifters was ∼18 km) was thus designed to obtain more information about the circulation on the continental shelf. Drifter trajectories from both "Lyap03" and "Lyap02" deployments allow a complete reconstruction of the shelf structures, indicating the presence of a cyclonic circulation analogous to the one further North-East in AVISO velocities (Figure 3 Right). The position of the hyperbolic point cannot be determined with the same accuracy as for the previous two deployments, since the "Lyap03" drifters were released relatively far from it. An approximate estimate of its position can be inferred only from the intersection of the reconstructed structures, which appear to have further migrated from their position on September 20.

The cyclonic structure is only partially revealed by ADCP measurements, since NIO remained quite strong on the continental shelf, as evidenced by the spiralling trajectories of the buoys in red. However, ADCP velocities in the south-western part of the continental shelf indicate the presence of a relatively intense southward jet. This is consistent with the "Lyap03" drifter trajectories, which, moreover, suggest that the jet extended southward past Cape Creus until it merged with the NC. Because of this jet, the western (repelling) and southern (attracting) LCSs represent offshore boundaries of a corridor along which continental shelf waters escape the GoL.

Comparing the detected structures with colormaps of AVHRR channel 4 data provides important support to our analysis (Figure 4). Unfortunately, due to cloud coverage within the period of drifter deployments, only data from September 15 are available. The figure

indicates a tight correlation between surface thermal features and drifter trajectories, evidencing that the *in-situ* detected LCSs are associated with observed physical structures, such as the front between warmer waters from the NC and colder waters from the shelf leaving the GoL along the western continental slope. The front marks the offshore limits of a tongue of cold coastal waters protruding southwards from the continental shelf. This cold tongue represents the surface signature of the corridor identified from the reconstructed LCSs, whose position and dimensions ($\sim$10 km wide in front of Cape Creus) can thus be further refined.

4. Discussion and Conclusions

Mapping transport structures in space and time is a challenging problem in coastal regions due to unreliability of altimetric data, noise and asynopticity in ADCP data, and only local information from drifter trajectories. During the Latex10 campaign, *in-situ* maps of LCSs in the western part of the GoL were successfully reconstructed using an adaptive sampling strategy that combines together these pieces of information. Integrating data from the different platforms was the key factor, since it allowed to go around the limitations of each individual measurement. FSLEs computed from AVISO velocities were used to initiate the sampling strategy, and to adjust the array deployments. Drifter trajectories allowed to identify key inconsistencies in the altimetry data and to correctly position the LCSs. Adjusting the initial position and the spatial arrangement of the arrays in subsequent deployments was fundamental for the *in-situ* detection, since the information on the dispersion properties of the flow provided by drifter trajectories, although very accurate, is extremely localized in space. The strategy allowed us to locate

very accurately even repelling LCSs (Figure 1 and 2, right), that are elusive to drifter experiments since particle trajectories diverge from them. Ship-based ADCP velocities, despite the strong signal associated with NIO, represented an important set of *in-situ* measurements to validate the interpretation of drifter trajectories, and to extend it over a wider area.

The three deployments allowed to reconstruct and follow the LCSs in the western part of the GoL for two weeks from September 12 to September 24, 2010. The detected hyperbolic point showed a south-westward migration along the continental slope with a translation speed of $\sim$5 cm sec^{-1}. This is slower than the average advection velocities in the region, providing an *in-situ* evidence that the requirements for the FSLE method are satisfied in coastal regions [*d'Ovidio et al.*, 2004], and thus FSLE analysis can be successfully applied for the study of coastal dynamics. The *in-situ* detected LCSs identified a $\sim$10 km-wide corridor in the south-western part of the GoL characterized by intense southward velocities. During September 2010, this corridor represents the pathway along which shelf waters leave the GoL, confirming on one hand the important role of the western part of the GoL in regulating cross-shelf exchanges [*Hu et al.*, 2011], and on the other hand, the importance of LCSs for the analysis of coastal transport. This will be further characterized and quantified in future studies by combining the information from the detected structures with the hydrographic measurements collected during the campaign. Recent advancements on LCS theory [i.e. *Haller*, 2011] may also suggest novel *in-situ* strategies.

The adaptive sampling strategy presented in this letter is a viable method to explore surface transport in coastal regions, and may provide significant information for guiding coastal environment management, as well as interventions in case of pollutant contamination when remote sensed information on the surface velocity field is not available or cannot be trusted. The case discussed in this paper, namely a single ship and a limited number of drifters, is what can be realistically expected to be available in many scenarios in which a mapping of surface coastal transport is critically time-constrained. This would be the case, for instance, of a rapid survey (i.e. few days) following an accidental pollutant release, or at the onset of a plankton bloom.

Coastal transport analysis exclusively from satellite derived FSLE will require some corrections to altimetry measurements in order to improve their accuracy in representing coastal circulation structures and their temporal evolution. These corrections could involve different strategies, including region-specific processing of raw satellite measurements, corrections using HF radar velocities, the addition of ageostrophic components not detected by altimetry (i.e. NIO), or novel high resolution altimetric instruments (SWOT mission). *In-situ* detected LCSs from this adaptive sampling strategy will represent an important term of comparison to validate such corrections.

Acknowledgments. The LATEX project is supported by the programs LEFE/IDAO and LEFE/CYBER of the INSU-Institut National des Sciences de l'Univers and by the Region PACA-Provence Alpes Côte d'Azur. The altimeter products were produced by Ssalto/Duacs and distributed by Aviso with support from Cnes. AVHRR data were supplied by Météo-France.

References

Abraham, E. R., and M. M. Bowen (2002), Chaotic stirring by a mesoscale surface-ocean flow, *Chaos: An Interdisciplinary Journal of Nonlinear Science*, *12*(2), 373–381, doi: 10.1063/1.1481615.

Aurell, E., G. Boffetta, A. Crisanti, G. Paladin, and A. Vulpiani (1997), Predictability in the large: an extension of the concept of lyapunov exponent, *Journal of Physics A: Mathematical and General*, *30*(1), 1.

Beron-Vera, F. J., M. J. Olascoaga, and G. J. Goni (2008), Oceanic mesoscale eddies as revealed by Lagrangian coherent structures, *Geophys. Res. Lett.*, *35*(12), doi: 10.1029/2008GL033957.

Bouffard, J., S. Vignudelli, P. Cipollini, and Y. Menard (2008), Exploiting the potential of an improved multimission altimetric data set over the coastal ocean, *Geophys. Res. Lett.*, *35*, L10,601.

Cotté, C., F. d'Ovidio, A. Chaigneau, M. Lévy, I. Taupier-Letage, B. Mate, and G. Christophe (2011), Scale-dependent interactions of mediterranean whales with marine dynamics, *Limnology Oceanography*, *106*(20), 219–232, doi: 10.4319/lo.2011.56.1.0219.

Csanady, G. (1982), *Circulation in the coastal ocean*, D.Reidel Publishing Company, Kluwer Group, Dordrech, Holland.

d'Ovidio, F., V. Fernández, E. Hernández-García, and C. López (2004), Mixing structures in the Mediterranean Sea from finite-size Lyapunov exponents, *Geophys. Res. Lett.*, *31*, L17,203.

d'Ovidio, F., J. Isern-Fontanet, C. López, E. Hernández-García, and E. García-Ladona (2009), Comparison between Eulerian diagnostics and finite-size Lyapunov exponents computed from altimetry in the Algerian basin, *Deep-Sea Res. I*, *56*(1), 15–31.

d'Ovidio, F., S. De Monte, S. Alvain, Y. Dandonneau, and M. Lévy (2010), Fluid dynamical niches of phytoplankton types, *Proc. Natl. Acad. Sci. U. S. A.*, *107*(43), 18,366–18,370, doi:10.1073/pnas.1004620107.

EEA (2010), 10 messages for 2010 – Coastal ecosystems, *EEA Message 9*, European Environmental Agency, Copenhagen.

Estournel, C., X. Durrieu de Madron, P. Marsaleix, F. Auclair, C. Julliand, and R. Vehil (2003), Observation and modeling of the winter coastal oceanic circulation in the Gulf of Lions under wind conditions influenced by the continental orography (FETCH experiment), *J. Geophys. Res.*, *108*(C3), 7–18, doi:10.1029/2001JC000825.

Haller, G., and G. Yuan (2000), Lagrangian coherent structures and mixing in two-dimensional turbulence, *Physica D: Nonlinear Phenomena*, *147*(3-4), 352 – 370, doi:10.1016/S0167-2789(00)00142-1.

Haller, G. (2011), A variational theory of hyperbolic Lagrangian Coherent Structures, *Physica D: Nonlinear Phenomena*, *240*(7), 574 – 598, doi:10.1016/j.physd.2010.11.010.

Haza, A. C., T. M. Ozgokmen, A. Griffa, A. Molcard, P.-M. Poulain, and G. Peggion (2010), Transport properties in small-scale coastal flows: relative dispersion from VHF radar measurements in the Gulf of La Spezia, *Ocean Dynam.*, *60*(4), 861–882, doi:10.1007/s10236-010-0301-7.

Hu, Z. Y., A. A. Petrenko, A. M. Doglioli, and I. Dekeyser (2011), Study of a mesoscale anticyclonic eddy in the western part of the Gulf of Lion, *J. Mar. Sys.*, *In Press, Corrected Proof*, doi:10.1016/j.jmarsys.2011.02.008.

Huthnance, J. (1995), Circulation, exchange and water masses at the ocean margin: the role of physical processes at the shelf edge, *Prog. Oceanogr.*, *35*(4), 353–431.

Kai, E. T., V. Rossi, J. Sudre, H. Weimerskirch, C. Lopez, E. Hernandez-Garcia, F. Marsac, and V. Garcon (2009), Top marine predators track lagrangian coherent structures, *Proceedings of the National Academy of Sciences of the United States of America*, *106*(20), 8245–8250, doi:10.1073/pnas.0811034106.

Largier, J. (2003), Considerations in estimating larval dispersal distances from oceanographic data, *Ecological Applications*, *13*(sp1), 71–89.

Lehahn, Y., F. d'Ovidio, M. Levy, and E. Heifetz (2007), Stirring of the northeast Atlantic spring bloom: A Lagrangian analysis based on multisatellite data, *J. Geophys. Res.*, *112*(C8), C08,005.

Lumpkin, R., and S. Elipot (2010), Surface drifter pair spreading in the North Atlantic, *J. Geophys. Res.*, *115*, doi:10.1029/2010JC006338.

Mancho, A. M., E. Hernandez-Garcia, D. Small, S. Wiggins, and V. Fernandez (2008), Lagrangian transport through an ocean front in the northwestern Mediterranean sea, *J. Phys. Oceanogr.*, *38*(6), 1222–1237, doi:10.1175/2007JPO3677.1.

Mezić, I., S. Loire, V. A. Fonoberov, and P. Hogan (2010), A New Mixing Diagnostic and Gulf Oil Spill Movement, *Science*, *330*(6003), 486–489, doi:10.1126/science.1194607.

Millot, C. (1990), The Gulf of Lions' hydrodynamics, *Cont. Shelf Res.*, *10*, 885–894, doi: 10.1016/0278-4343(90)90065-T.

Olascoaga, M. J., I. I. Rypina, M. G. Brown, F. J. Beron-Vera, H. Kocak, L. E. Brand, G. R. Halliwell, and L. K. Shay (2006), Persistent transport barrier on the West Florida Shelf, *Geophys. Res. Lett.*, *33*(22), doi:10.1029/2006GL027800.

Petrenko, A., Y. Leredde, and P. Marsaleix (2005), Circulation in a stratified and wind-forced Gulf of Lions, NW Mediterranean Sea: in situ and modeling data, *Cont. Shelf Res.*, *25*, 7–27, doi:10.1016/j.csr.2004.09.004.

Resplandy, L., M. Levy, F. d'Ovidio, and L. Merlivat (2009), Impact of submesoscale variability in estimating the air-sea CO2 exchange: Results from a model study of the POMME experiment, *Global Biogeochem. Cy.*, *23*, doi:10.1029/2008GB003239.

Shadden, S. C., F. Lekien, J. D. Paduan, F. P. Chavez, and J. E. Marsden (2009), The correlation between surface drifters and coherent structures based on high-frequency radar data in Monterey Bay, *Deep-Sea Res. II*, *56*(3-5), 161–172, doi: 10.1016/j.dsr2.2008.08.008.

Schroeder, K., A. C. Haza, A. Griffa, T. M. Ozgoekmen, P. M. Poulain, R. Gerin, G. Peggion, and M. Rixen (2011), Relative dispersion in the Liguro-Provencal basin: From submesoscale to mesoscale, *Deep-Sea Res. I*, *58*(3), 209–228, doi:10.1016/j.dsr.2010.11.004.

SSALTO/DUACS User Handbook (2010), *(M)SLA and (M)ADT Near-Real Time and Delayed Time Products*, cLS-DOS-NT-06.034.

Waugh, D. W., and E. R. Abraham (2008), Stirring in the global surface ocean, *Geophys. Res. Lett.*, *35*(20), doi:10.1029/2008GL035526.

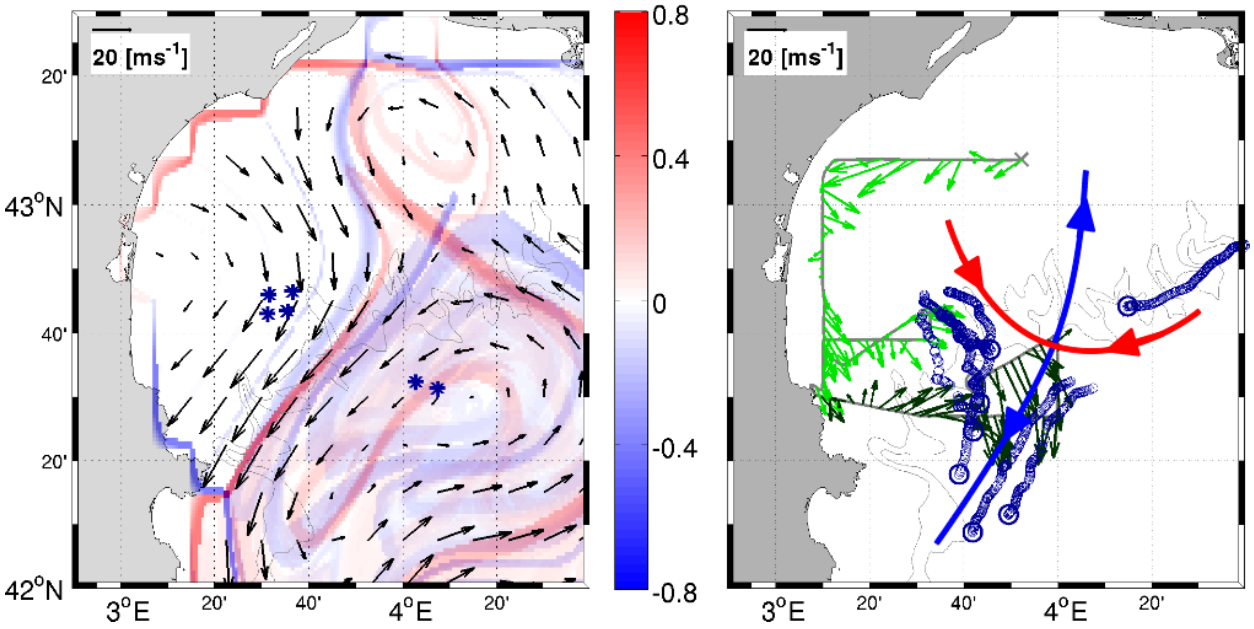

Figure 1. (Left) AVISO geostrophic velocities (vectors), and FSLEs (s^{-1}; shaded) on September 14; initial position of "Lyap01" drifters (blue stars) on September 12 (the initial position of the third drifter with a 50m-depth drogue is out of the figure domain). (Right) Drifter trajectories and 15m-depth ADCP velocities from September 12 to 14. Larger circles indicate the final position of the drifters on September 14. ADCP velocities from different days are plotted from light to dark green. Vectors are plotted one every ten. In red and blue are the reconstructed repelling and attracting LCSs, respectively.

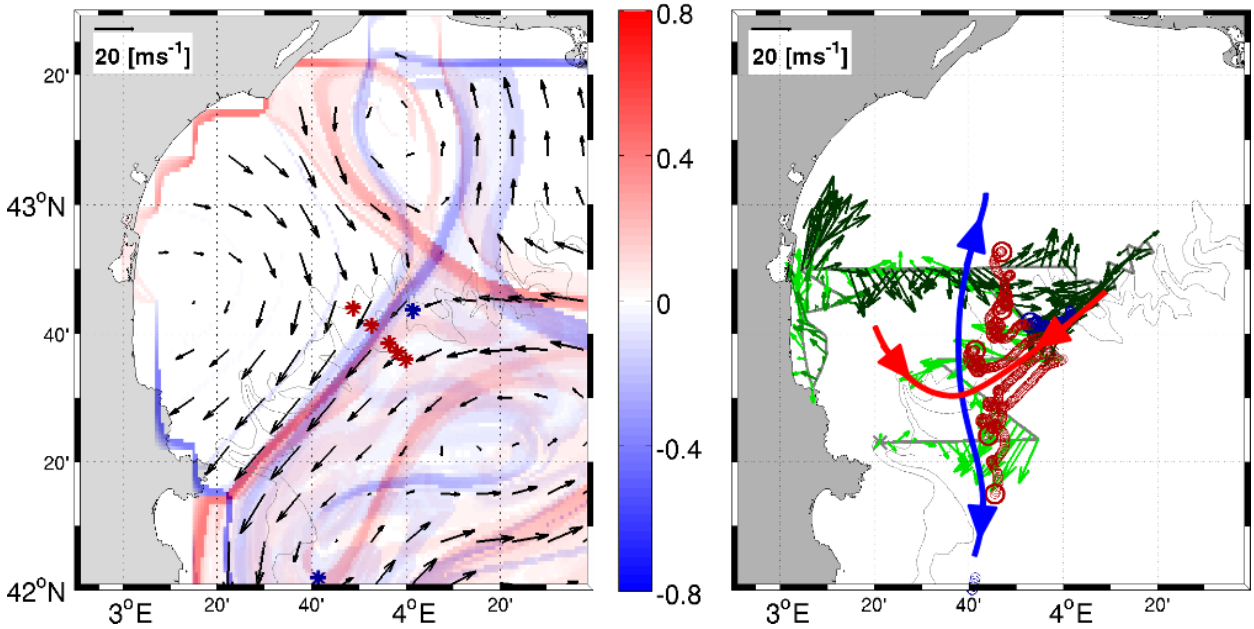

Figure 2. Same as Figure 1 but for the "Lyap02" experiment. AVISO velocities and FSLEs are from September 20. The drifters (red) were deployed on September 18.

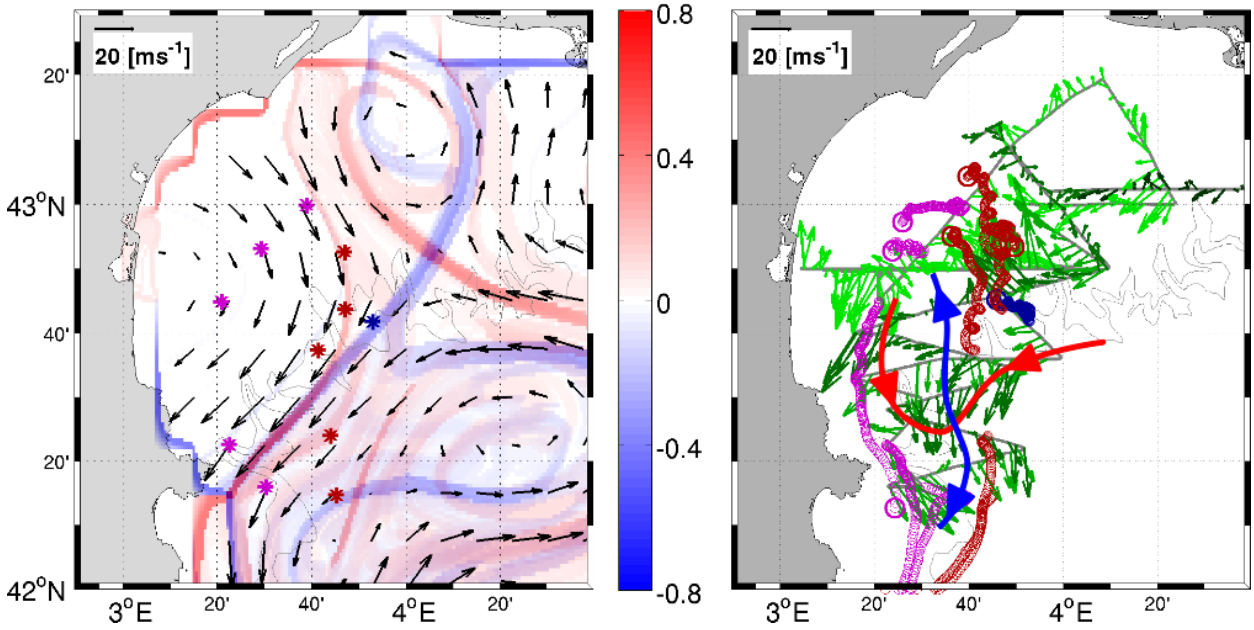

Figure 3. Same as Figure 1 but for the "Lyap03" experiment. AVISO velocities and FSLEs are from September 24. Drifters in magenta were deployed on September 21; drifters in red are from the "Lyap02" deployment.

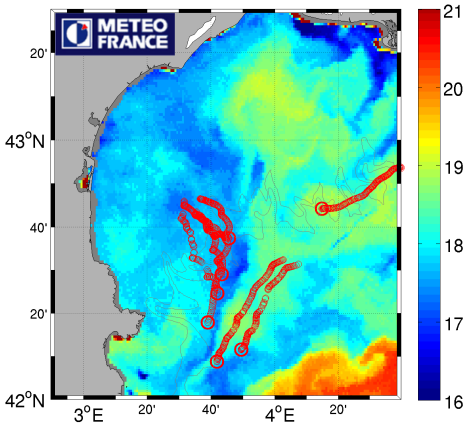

Figure 4. "Lyap01" drifter trajectories (red) superimposed to AVHRR Channel 4 data (proxy for SST; shaded) for September 15. The data were provided by Météo-France.